INTERFERENCE DUE TO HYDROMETEOR SCATTERING ON HORIZONTALLY POLARIZED SUPER HIGH FREQUENCY (SHF) SIGNAL PROPAGATION IN A TROPICAL LOCATION.

ROTIMI CORNELIUS OKEOWO
(PHY/98/1874)

A THESIS SUBMITTED IN PARTIAL FULFILMENT OF THE REQUIREMENT FOR THE AWARD OF THE DEGREE OF MASTER OF TECHNOLOGY (M.TECH.)

IN

COMMUNICATION PHYSICS

DEPARTMENT OF PHYSICS
FEDERAL UNIVERSITY OF TECHNOLOGY,
AKURE, ONDO STATE, NIGERIA.

CERTIFICATION

I certify that Mr. C.O Rotimi has carried out this work under my supervision in the Department of Physics, Federal University of Technology, Akure, Ondo state Nigeria.

15/9/08

Prof. M.O Ajewole. B.Sc., M.Sc. (Ilorin), PhD (Akure)

Department of Physics

Federal University of Technology

Akure, Ondo state Nigeria.

DEDICATION

This work is dedicated to the glory of Almighty God.

ACKNOWLEGEMENT

The completion of this work was made possible by some men of good will, especially those who offered useful and relevant information during the course of my investigation.

I am grateful to Amighty God for His grace that kept me throughout the period of this research work.

I am mostly grateful to my supervisor, Prof. M.O Ajewole for his encouragement, useful suggestions, thorough supervision and his assistance in making his library available for me in order to make this work a success. His support in providing the most recent journals and conference papers that are relevant to this dissertation enabled me to carry out this work with the most recent techniques. Also, his readiness to attend to any of my complaint anywhere is highly appreciated.

I cannot but acknowledge with thanks the encouragement received from Dr. M.T Babalola.

I wish to show sincere appreciation to Messrs J.S.Ojo, Kunle Adediji, S.A Oni and A.O Awodun for their readiness to assist in the course of this research.

I am also grateful to my wife, Mrs. H.T Rotimi who stood by me throughout the period of this work.

TABLE OF CONTENTS

CHAPTER THREE

RESULTS AND DISCUSSION

CHAPTER FOUR

LIST OF FIGURES

ABSTRACT

This report presents the result of the computation of intersystem interference due to hydrometeors using the simplified Capsoni Three Dimension (3-D) model when horizontally polarized super-high frequency signals propagates through thunderstorm rain type in Nigeria. The results obtained show that transmission loss increases with increasing terrestrial transmitter to common volume distance indicating decreasing probability of severe interference on the satellite system. Also, the frequency characteristics of the transmission loss when transmitter antenna gain is 45dB and time percentage unavailability is greater or equal to 0.01% (≥ 0.01) shows that transmission loss varies from 121.28dB to 135.58dB for short path lengths while for the long path lengths, it varies from 159.4 to 166.35dB. In addition, evaluation of the effective transmission loss shows that additional rain attenuation along the path will severely weaken the received satellite signal, which may lead to acute signal outage during occurrence of heavy and intense tropical precipitation. However, the results of the present work are in good agreement with those of the previous researchers particularly for Nigeria which utilized vertical polarization.

CHAPTER ONE
INTRODUCTION

The recent rapid growth in telecommunication systems needs to be critically studied as more communication satellites have been launched into space for the provision of telecommunication and other communication services. Many new technologies like the use of VSAT and MSAT terminals for wireless internet data transfer, digital visual display (DVD), fixed and mobile telephony among others which are based on satellite communication also continue to spring up almost everyday and more will still be available in the nearest future. The existence of these services has led to the congestion of spectrum, hence technique of frequency re-use whereby a terrestrial radio relay link will use the same frequency as the earth station link is now being employed to increase the number of services without increasing the bandwidth.. Thus, producing a correspondingly greater likelihood of interference. Interference is usually responsible for the decrease of the signal-to- noise (S/N) ratio at the interfered terminal and this could lead to link outage. The maximum interference occurs for geometries for which there is considerable overlap between two antenna mainlobes.

The interference that occurs for several geometries is due to the omni-directional nature of the precipitation scatter (Thurai, 1994). This is so since the signals intended for one microwave system may be scattered by hydrometeor to cause interference in other microwave system operating at the same frequency. Therefore, assessing the degree of such interference on statistical term is extremely important for the correct design of communication systems operating at microwave frequency (Capsoni, et al, 1997).

The term hydrometeor refers to the products of condensed water vapour in the atmosphere usually observed as rain, hail, ice, fog, cloud or snow. The most important of these hydrometeors to radio wave propagation is rain. An electromagnetic wave propagating through a region containing raindrops usually suffers two types of attenuation; part of the energy is absorbed by raindrops and transformed to heat which is known as absorption while another part is scattered in all directions. This may be forward scattering or back scattering (Medeiros Filho et al, 1986).

For bistatic intersystem interference to be observed, there must be precipitating particles such as rain, atmospheric particles, ice particles and other hydrometeors in the common volume intersected by the two antenna beams of the independent communication links. Hence, the fact that these hydrometeors originate from high altitudes makes their scattering of radio waves omni-directional (Ajewole, et al, 1999). Therefore, the investigation of hydrometeor scattering in the tropical environment that is known for high rainfall intensity is very important.

In the tropical region, convective activity is often the prevailing climatic condition, in its climates since strong vertical air motion gives rise to large scale mixing of frozen, liquid and partially melted hydrometeors. Convection also results in super cooled drops or wet hail to be present at large heights, giving rise to high reflectivity values. For the prediction of interference, parameters such as electrical system, meteorological variables etc are needed to calculate the transmission loss due to hydrometeor scatter between two microwave stations. The level of interference also depends on the specific geometry, the characteristics of the two-antenna systems and the structure of rain in the medium, among others.

Among the numerous models proposed for the prediction of interference due to hydrometeor, Capsoni, et al; (1987); Capsoni and D'amico, (1997) and Awaka and Oguchi, (1982) which are based on the assumption of an exponential rain cell model are quite unique. They assumed that the horizontal structure of rain is the same in all rainfall zones (Ajewole, et al, 2005b). Also, the International Telecommunication Union (ITU) and the International Radio Consultative Committee (CCIR) as well as European Cooperative Program (COST 210, 1991) have also developed new propagation models for interference. These models however have some limitations which include yielding excessively large rain cell radius when rain intensity is $\leq$ 6mmh^{-1}, over-estimating the attenuation of the wanted signal in the computation of the effective transmission loss, non-inclusion of the relationship between the reflectivity factor and the attenuation on one hand and the assumption of a fixed rain cell position in space, among others. For these reasons and the enormity of computation involved in the complete 3D model, the simplified version of the 3D model of Capsoni et al. (1997) has been used in this study to predict the cumulative distribution of transmission loss.

1.1 The scope of the study

In this report, investigation of hydrometeors that affect the availability of the wanted channels in a tropical location is investigated. Emphasis is on the availability of satellite channels receiving interfering signals from terrestrial microwave relay link operating at the same frequency as a result of hydrometeor scatter in the common volume formed by the intersection of their antenna beams. The study is limited to the frequency range of 4-35GHz where there is high degree of frequency sharing and co-ordination between the terrestrial and earth – space systems. The study also focuses attention on the possibility of a terrestrial microwave radio interfering with the

reception of satellite traffics over both short (≤50Km) and long (≥ 50Km) paths in a tropical region. Probability levels ranging from about 10^{-3}-1% are considered. The mean annual point rain rate P(R) measured at Ile-Ife, Nigeria is used. Convective thunderstorm rain type is assumed since this is prevalent in the region. The interfering signals are assumed to be horizontally polarized since this also contributes to the interfering of signals transmitted via the two antennas.

1.2 Statement of objective of the research.

The specific objectives of the research are to:

a. Compute the statistics of the interference (Transmission loss) arising from transmission of horizontally polarized signal between a terrestrial radio relay link and earth-satellite station operating in the frequency band of 4-34GHz in Nigeria.

b. Use the information obtained in such statistics to predict occurrence of signal outages during transmission through high intensity rainfall occurrence in Nigeria.

CHAPTER TWO

2.0 BASIC CONCEPTS

In this section, the basic concepts needed for the evaluation of interference due to hydrometeor scattering is considered. The basic input parameters include the link geometry, system and meteorological parameters. For the geometric parameters, information about the antenna separation (Km), common volume height or distance from the transmitter to common volume – receiver among others are needed. The meteorological parameters needed include information such as the horizontal and vertical structure of rain, mean freezing height during rainy conditions, mean reflectivity to height profile around the melting layer, width of rain cell as a function of rain rate, the drop size distribution, path attenuation, and so on. The system parameters required include elevation angle of antenna, relative height of antenna, channel polarization, antenna gains and beam-width, efficiency factor, radiation pattern, frequency range, parameters for estimating attenuation along the path, and so on.

Let us consider an electromagnetic energy radiated by a transmitting antenna. Let us also assume that this illuminates a region of space, which is intercepted by atmospheric precipitation. Using this same region to view the antenna beam of a receiving terminal operating at the same microwave frequency, interference may occur. The scattered wave arriving at the receiving antenna is composed of a very large number of elementary waves. Each of the wave is generated from a single hydrometeor in the common volume and assuming that each elementary wave is different from one another in size, shape, location and movement. Also, all these

waves have undergone attenuation while travelling on slightly differing paths. Fig.2.1 is a typical sketch of hydrometeor scatter. The path geometry of hydrometeor scatter

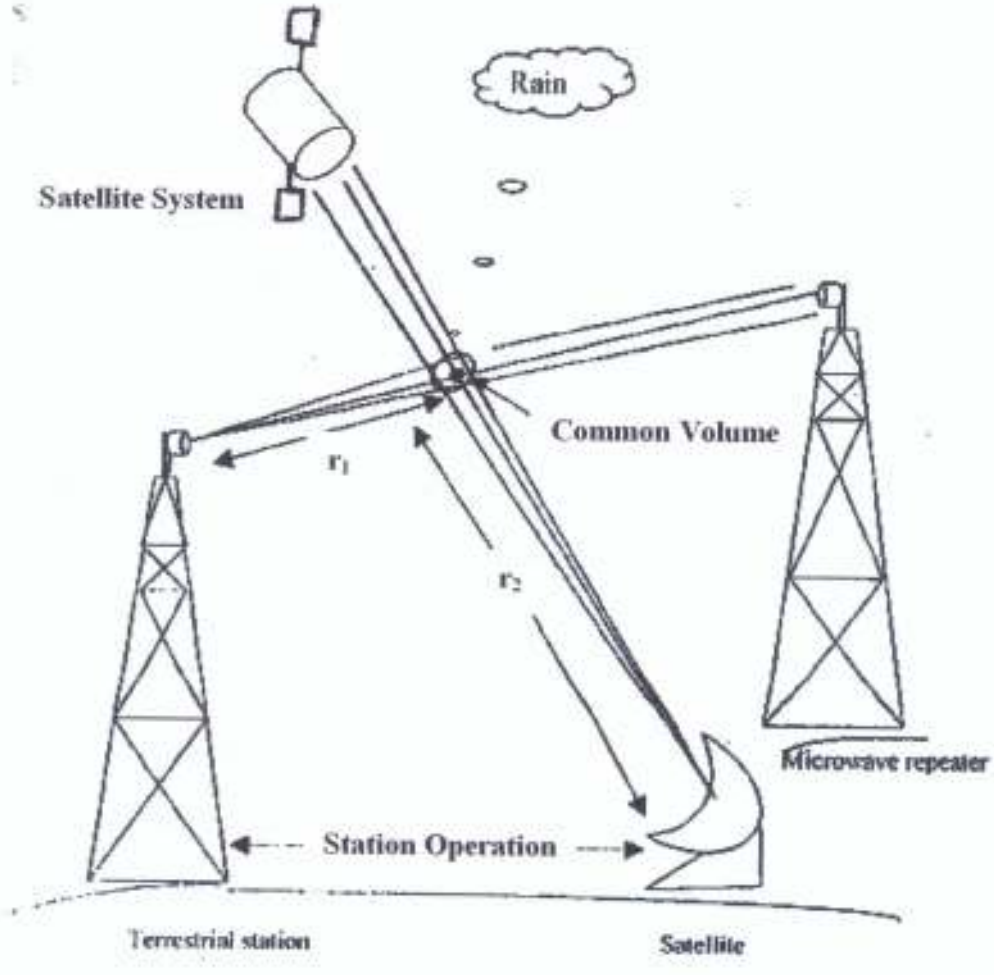

Fig. 2.1 Hydrometer scatter propagation geometry from a terrestrial system to an Earth-space system operating at the same frequency.

interference is usually defined in terms of the station separation, their projection to the common volume as well as their relative bearing. From Fig.2.1, there is the presence of scatterers in the common volume, that is, the region of space defined by the intersection of the two antenna beams, part of the energy propagating along r_1 is redirected along r_2, hence leading to interference in the satellite receiver.

2.1 THE CHARACTERISTIC EQUATION–The Bistatic Radar Equation (BRE)

Crane, (1974) developed an equation to evaluate the amount of (wanted) energy that reaches the Earth-space system (receiver) – the Bistatic radar equation. It was analysed in terms of the ratio of signal power in the two systems. If the multiple scattering by atmospheric particles are neglected, the BRE can be expressed as

$$\frac{P_t}{P_r} = G_t(t)G_r(o)\frac{\lambda^2}{(4\pi)^3}\int_{cv}\frac{F_t(\theta_1\phi_1)F_r(\theta_2\phi_2)A_t(r_1)A_r(r_2)A_z}{r_1^2 r_2^2}dv\int_0^{\infty}N(D)\sigma_s(i,0,D)dD \qquad 2.1$$

where P_t and P_r are the mean power (Watts) transmitted and received along the axis of the main antenna beams respectively, $F_{t,r}(\theta,\phi)$ denotes the directivity function of the antenna systems from which the effective areas are calculated. $A_{t,r}(r_1,r_2)$ represents the attenuation along the paths from and towards the common volume, while Az is the attenuation due to gaseous absorption, $G_{t,r}$ are the transmitter and receiver antenna gains, λ is the wavelength of the radio signal, $r_{1,2}$ are the separation distance from the transmitter to the common volume and from the common volume to the receiver, D is the particle equivolumic diameter, N(D) is the particle number density in a diameter interval dD, σ_s is the total scattering cross-section of particles with diameter D inside the common volume and it is related to the reflectivity factor, point rain rate R and the complex refractive index of the rain drops. At frequencies above 10GHz, and as raindrops size gets bigger than 3mm, correction for Rayleigh scattering must be taken

into consideration. To evaluate the transmission loss, L, the inverse log of equation (2.1) will be taken to yield,

$$L = 10\log_{10}\frac{P_t}{P_r} \qquad 2.2$$

The evaluation of equation (2.2) depends on several factors such as the link geometry, electrical and meteorological parameters and these are also interdependent, as such, it is very cumbersome to evaluate such equation at once. From the physical point of view, extracting all the parameters from the integral part of equation (2.1) shows that the common volume can be reduced to a single point corresponding to the intersection of the two antenna axes where the total scattering cross-section is evaluated. This is called the pencil beam approximation.

2.2 THE SIMPLIFIED FORM OF THE 3D BRE.

Using the pencil beam approximation approach, where the common volume is assumed to be very small compared to the distances r_1 and r_2 in equation (2.1), A_t and A_r are also assumed independent of their positions in the common volume, and the total scattering cross-section is also assumed constant within the common volume, hence, the simplified form of equation (2.1) can be expressed as

$$\frac{P_r}{P_t} = \frac{A_t(r_1)A_r(r_2)A_v G_t(\theta)G_r(\theta)\lambda^2\delta_{bi}}{(4\pi)^3 r_1^2 r_2^2} \times \int_0^{\infty} F_t(\theta_1,\phi_1)F_r(\theta 2,\phi 2)dv \qquad 2.3$$

The symbols are as defined in equation (2.1) while δ_{bi} is defined as the scattering cross-section per unit volume of precipitation and this replaces the second integral term on the far right of equation (2.1). This quantity depends on the frequency and polarization of the incident and scattered waves and on the value of refractive index, size and shape of the hydrometeor among others.

The single particle scattering cross-section per unit volume can be evaluated numerically using the complete Mie solution or Rayleigh approximation. Hence, at frequencies less than 10GHz, it is expressed as

$$\delta_{sc} = 10^{-18}\frac{\pi^5}{\lambda^4}\left|\frac{\varepsilon-1}{\varepsilon+2}\right|^2 Z \qquad 2.4$$

where λ is the wavelength in metres and ε is the permittivity of the medium (that is frequency, temperature and particle phase dependent), z is the radar reflectivity in mm^6m^{-3}. Using the power law relation,

$$z = aR^b \qquad (2.5)$$

where R is the rain rate (mm/h), a and b are constants which are readily available (Ajayi and Owolabi, 1987). Then,

$$Z = 10\log z \qquad (2.6)$$

z can be obtained from equation (2.5).

For tropical thunderstorm rain type, assumed in this study, the parameters a and b of equation (2.5) are a = 464 and b = 1.31 (Ajayi and Owolabi, 1987).

2.3 THE MODIFIED FORM OF THE SIMPLIFIED BRE

Using the assumptions of the contributions from the elementary volumes forming the common volumes, equation (2.3) can be modified in terms of the transmission loss L, into (Ajewole, 2003, Ajewole and Ojo, 2005a)

$$I = P_t - P_r = K_T + A_g - M + (S - Z + A) \qquad (2.7)$$

All the terms are in decibel. S is the allowance for Rayleigh scattering at frequencies greater than 10GHz and is given as;

$$10\log S = R^{0.4}10^{-3}\left[4(f-10)^{1.6}\left(\frac{1+\cos\theta_s}{2}\right)+5(f-10)^{1.7}\left(\frac{1-\cos\phi_s}{2}\right)\right] \qquad (2.8)$$

where f is the frequency (GHz) and ϕ_s is the scattering angle. Note that 10logS = 0 if $f \leq 10$GHz. Other symbols in equation (2.7) are defined thus: A_g is the extra attenuation due to gaseous absorption, P_t and P_r are the transmitted and the received power, M is the polarization decoupling factor and A is the slant path rain attenuation from the transmitter to the common volume and from the common volume to the satellite receiver. This is calculated using the power law relationship between rain rate and attenuation and can be expressed as;

$$A_H = K_H R^{\alpha_H} \tag{2.9}$$

The subscript H refers to the horizontal polarization and the constant parameters K_H and α_H for calculating attenuation A are shown in Table (2.1) for the respective frequencies investigated in this study, Z has been calculated in (2.5) and (2.6) and the term K_T is of the form;

$$K_T = 10\log\left[\frac{G_1 G_2 \pi^2}{64^3 \lambda^2}\left|\frac{m^2-1}{m^2+1}\right| \times 10^{18}\int \frac{F_1(\theta_1\phi_1)F_2(\theta_2\phi_2)}{r_1^2 r_2^2}dv\right] \tag{2.10}$$

The symbols are as defined in equation (2.1) and dv is the elementary volume. (Capsoni and D'Amico, 1997)

Table 2.1: Regression coefficients K and α of the power law expression for the thunderstorm rain type (Ajewole, et al, 1999). H = horizontal polarization.

Frequency (GHz)	K_H	α_H
4.0	7.74×10^{-4}	1.0305
6.0	3.28×10^{-3}	1.0760
8.0	8.89×10^{-3}	1.1269
10.0	0.018	1.1332
12.0	0.0302	1.1130
15.0	0.0528	1.0756
20.0	0.0963	1.0450
25.0	0.1463	1.0340
30.0	0.2045	1.0170
35.0	0.2700	0.9920

2.4 OVERVIEW OF SOME EXISTING MODELS FOR PREDICTING INTERFERENCE

Many models and prediction techniques have been adopted for determining interference due to hydrometeor scatter between two independent microwave stations. Among the most widely used models are: International Radio Consultative Committee as reported in COST 210 (1991), International Telecommunication Union Radio Committee (ITU-R) model, Capsoni's exponential rain cell model, Awaka model, Gaussian profile model, Crane model and the simplified 3D cell model among others. Among the pack, the Capsoni model is unique because it demonstrated that the horizontal structure of rain is the same in all rainfall climatic zones. The difference among rainfall zones lies in the measured cumulative distribution of rainfall rates of the ITU-R. Some of the most widely used model are also described.

2.4.1 THE CCIR MODEL

The International Radio Consultative Committee hydrometeor scatter model is intended to predict transmission loss statistics from rainfall rate statistics. It is based on two fundamental assumptions: (i) that scattering occur only within rain cells having circular cross section and whose diameter depends on the rainfall rates inside the cells and that attenuation occurs inside as well as outside the cell, but only below the rain height. Statistics of measured data on the 11-18GHz (COST 210, Report 569, 1991) range seems to show reasonable agreement with the predictions on the basis of the model. At higher frequencies (30GHz and above), however, larger deviations have been observed. (ii) That the rain height is the time-invariant and this determines whether the scattering will occur in the rain or in the ice region. The limitations of the model however are:

(i) Only coupling between a narrow-beam earth station and a distant terrestrial radio relay station is considered.

(ii) Exact intersection of antenna axes is assumed while the side-lobe coupling is not considered.

(iii) No side scatter is included in the analysis, only forward and back scatter are considered.

The CCIR model was later modified and the resulting expression for the determination of transmission loss at frequency f, is

$$L = 168 + 20\log r - 20\log f - 13.2\log R - g_T + 10\log A_b - \log C + r + \gamma_o d_o + \gamma_v d_v \qquad (2.11)$$

where r is the distance between the region of maximum scattering and the location of an earth station, R is the surface rainfall rate (mmh^{-1}) for the required climatic region, g_t is the gain of the terrestrial station antenna, A_b is a correction factor for non-Rayleigh scattering, C is the effective scatter transfer and is expressed as;

$$C = \frac{2.17}{\gamma R^{\beta}}\left[1 - 10^{-\gamma R^{\frac{\beta}{4}}}\right] \quad f > 4GHz \qquad (2.12a)$$

$$f \leq 4GHz \qquad (2.12b)$$

$$\gamma_R = KR^{\alpha} \qquad (2.13)$$

$\gamma_o d_o + \gamma_v d_v$ are the atmospheric attenuation for oxygen and water vapour respectively.

$$d_r = 3.5R^{0.8} \text{ km} \qquad (2.14)$$

$$l = 63kR^{\alpha-0.5} \cdot 10^{-(R+1)0.19} \quad \text{dB} \qquad (2.15)$$

2.4.2 GAUSSIAN PROFILE MODEL

It uses non-orthogonal gaussian function expansion of vertical reflectivity profiles. In addition, it allows quick calculation of the bistatic radar cross-section in hydrometeor scatter problem solving arbitrary reflectivity profiles. In particular, it allows scattering

from melting band and ice regions to be included in the cross-section calculation. This model however lacks a physical basis.

2.4.3 THE CRANE MODEL

Crane (1974) investigated the bistatic scatter from rain using weather radar instrument in the Avon-to-Westford (Coventry). He was the first to undertake detailed measurement of the effect, and his work remained for a long time the basis of the ITU-R prediction method (Ajewole, et al, 1999). Transmission loss was estimated for the bistatic scatter paths, which was computed using the weather radar data, the bistatic radar equation, and a model for the scattering cross-section per unit volume of rain based upon Rayleigh scattering by an ensemble of water sphere. The model predicts low values for all rain conditions.

2.4.4 THE ITU-R MODEL

This model predicts the distribution of rainfall rate in a locality. It investigates the problem of hydrometeor interference by assuming the 3-D exponential rain cell model of Capsoni et al (1997). The model offers possibility of predicting the statistics of many propagation parameters such as attenuation, interference by rain scattering, etc, which are determined by the rain cell characteristics and their frequency of occurrence. The model has some limitations such as yielding excessively large rain cell radius when rain intensity is less or equal to $6mmh^{-1}$, over-estimating the attenuation of the wanted signal in the computation of the effective transmission loss. Also, the non-inclusion of the relationship between the reflectivity factor and the attenuation on one hand and the assumption of a fixed rain cell position in space is another limitation of the model.

2.4.5 THE 3D CELL MODEL

Due to the limitations associated with models described earlier, a three-dimensional rain cell model (3D cell model) has been developed to examine a non-fixed cell situation and to improve on the afore-mentioned limitations.

Hydrometeor scattering is observed when a rain cell passes through the common volume, which is defined by the intersection of the antenna main beams. At any time, the transmission loss can be computed by the BRE if the location and structure of the cell are specified. The computed transmission loss may vary with time because of the movement of the rain cell and because of the temporal change in the rain cell structure. For simplicity, this study assumes that the rain cell structure does not change in time. Then the temporal changes in the transmission loss occur only because of the movement of the rain cell.

Hydrometeor scattering is observed when a rain cell overlaps with the common volume. After the rain cell moves away from the common volume, no hydrometeor scattering is observed for a while. Then there comes another rain cell with different size and intensity into the common volume, and hydrometeor scattering resumes. When this process continues for a long time all possible values of the transmission loss are obtained. The ergodic hypothesis (Mismie and Waldteufel, 1980) enables us to compute the probability of observing the values of transmission loss. Hence, the cumulative distribution of the transmission loss can be computed. The procedure above requires specifications of the rain cell structure and the movement of the rain cell.

2.4.6 RAIN-CELL STRUCTURE (Spatial structure of rain cell)

The spatial structure of precipitation rate (mmh^{-1}) in both the vertical and horizontal direction is needed to compute statistics of transmission loss. The vertical structure of precipitation assumes that rainfall rate is vertically homogeneous up to the rain height. The radar reflectivity Z is a useful parameter for defining the vertical structure of rain. The vertical structure of precipitation is assumed constant up to the 0°C isotherm height below which is the rain region where attenuation and scattering of the wanted and the interfering signals occur. Beyond the 0°C, is the ice region where Z decreases at the rate of 6.5dB/Km (Ajewole, 2003) and attenuation is small. Z is climate and region dependent. It varies in the temperate region, while it is relatively stable in the tropical climate (Ajayi and Barbalisca, 1990). The physical rain height on the other hand is a more practical quantity for defining the height of the rain region especially for rainy conditions. The expression proposed by the ITU-R for mean 0°C isotherm height (h_o) which can be equated to the mean 0°C isotherm height (h_{FR}) during rainy conditions in the tropical region is;

$$h_{FR} = 5.0Km \qquad 0 < \phi \leq 23 \qquad (2.16a)$$

ϕ is the latitude of the locations. Due to the over-estimation of the h_{FR} by this model worldwide, Ajayi and Barbalisca (1990) used radiosonde data to propose a relationship for h_{FR} for Nigeria. This relationship depends weakly on the rain rate value averaged over a 2hr period, that is; 1hr before and 1hr after the launch of the radiosonde. It is expressed as;

$$h_{FR} = 4.67 + 6 \times 10^{-3} R \qquad (2.16b)$$

An example of the horizontal cross-section of a rain cell is shown in figure 2.2. The rain cell has a cylindrical symmetry. Within the horizontal cross-section, the rainfall

rate is assumed to vary exponentially at point x and y (Capsoni et al, 1987) and is expressed as;

$$R(x,y) = R_m e^{-\frac{r}{r_0}} \tag{2.17}$$

where r is the radial distance with coordinate (x,y) from the rain cell centre, R_m is the maximum rainfall rate and r_o is the parameter characterizing the cell size.

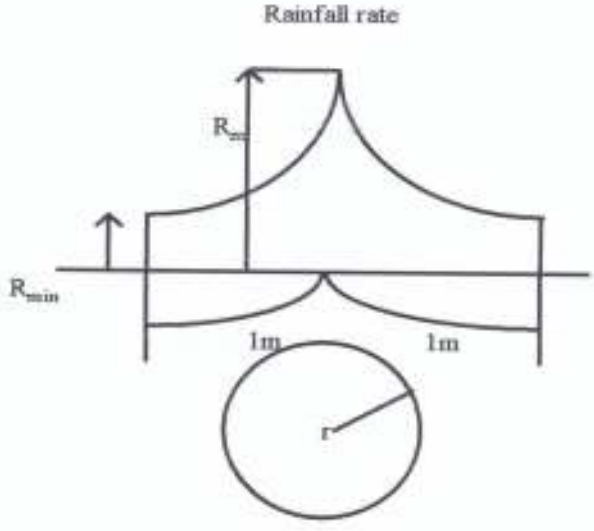

Fig.2.2: Horizontal cross-section of a rain cell

It is necessary to truncate r at a certain distance r_m where the rain intensity is maximum (R min). R_{min} occurs at the distance at which $r = r_o$ and where r is greater than r_m there is no rain. The expression can be written as;

$$r_o = \frac{r_m}{\ln \frac{R_m}{R_{min}}} \tag{2.18}$$

According to Capsoni and D'Amico (1997), for any range of peak rain rate, rain cells present well – defined exponential distribution of sizes regardless of the range of R_m considered. A probability density is then attached to this exponential distribution, which is a function of the conditional average radius (size) of the rain cells. This conditional average radius (size) is expressed as;

$$r_o(R_m) = 1.7\left[\left(\frac{R_m}{6}\right)^{-10} + \left(\frac{R_m}{6}\right)^{-0.26}\right] \tag{2.19}$$

2.4.7 RAIN- CELL MOVEMENT

Rain Cells are assumed to have constant velocity. Let us consider identical rain cells in the first place. Though the cells are identical in structure, the shortest distance between the centre of the cell and the centre of the common volume, which is a similar concept to the impact parameter in the collision theory varies with each cell. The closest distance is assumed distributed uniformly in statistical senses.

In actual fact, the centre of the common volume is located at a fixed point whereas the rain cells move about. However, since the rain cells are assumed to be identical and are also assumed to have the same velocity, the actual situation can be regarded as equivalent to the following situation in a statistical sense. A rain cell is fixed in space whereas the centre of the common volume moves about uniformly on a horizontal plane in the rain cell. We also assume that each type of rain cell contains infinite

number of identical cells crossing the common volume. Values of the transmission loss vary depending on the position of the centre of the common volume in the rain cell. The above statistically identical situation enables us to compute the cumulative distribution of transmission loss.

2.4.8 THE SPATIAL DENSITY

The exponential shape, the type of distribution of rain cell sizes, and the conditional average radius are valid in any location. Hence, any meteorological rain environment can be modelled by a group of isolated rain cells having different peak rain rates and sizes by attaching an appropriate statistical weight.

This fact enables us to utilise the Excel shape model of the horizontal structure of rain. The difference from one location to another is reflected in the probability of occurrence of a rain cell which is represented by the cell spatial density; that is the number of cells per square kilometre and per unit peak rain rate, R_m and r_0. It is expressed as;

$$N(r_0, R_m) = N^*(R_m)\exp\left[\frac{-r}{r_0(R_m)}\right] \qquad (2.20)$$

Where $N^*(R_m)$ is the spatial density of cells with peak rain rate R_m no matter the value of r_0. This parameter is related to the cumulative distribution of the point rain rate, which is location dependent, and is easily available from the measurement at the location of interest or from ITU – R rain climatic zones.

In terms of area probability, Capsoni et al., (1987), further simplified $N^*(Rm)$ by setting the probability P (R) of finding R(x,y) of equation (2.17) greater than R', and proportional to the geometric area over which R is greater than R', thus for a third order derivative of R_m;

$$N^{*}(R_m) = \frac{-1}{4\pi R_m^2 v_t(R_m)} \left| \frac{d^3 P(R)}{d(\ln R)^3} \right|_{R=R_m} \quad (2.21)$$

A log – power – law expression was then adopted to define the measured values of P(R). The expression proposed is given as;

$$P(R) = P_o \ln\left(\frac{R'}{R}\right)^K \quad (2.22)$$

P_o and K can be obtained by interpolation from cumulative distribution of the measured point rain rate P(R) or from the ITU – R (1999) rain climatic zones. R′ is normally assumed to be about four times the highest rain rate at the location of interest. The summary of P_o, R′ and K for Ile-Ife, Nigeria is shown in Table 2.3. The average water vapour density of $20g/m^3$ (Ajewole et al. 1999) was assumed to calculate attenuation due to absorption by atmospheric gases while water temperature of 20°C was assumed to calculate refractive index of water using the method of (Ray, 1972).

Table 2.3: Power law parameters for the local cumulative probability density for thunder storm convective rain type for the location considered and the Z – R relation.

Location	P_o	R′	K	$Z=aR^b$
Ile-Ife, Nigeria	5.91×10^{-4}	624	4.5585	$461R^{1.31}$

2.5 INPUT PARAMETERS USED FOR MODELLING

The modelling of the modified 3D cell model requires some input parameters, which include the local meteorological information of the location and the geometrical and electrical properties of the link. Inputs for electrical characteristics of the link include antenna gains, antenna polarization, 3dB beam widths, operating frequency and polarization decoupling factor M. The geometrical information with respect to a common volume reference system include; antenna pointing and distance between the stations. The meteorological information required includes 0°C isotherm height, cumulative distribution of point rainfall rate P(R) and water vapour density. The additional input information needed are the relationship between the specific attenuation and rain rate between radar reflectivity and rain rate and the deviation from Rayleigh scattering.

In this study, the lognormal distribution for the drop size distribution (dsd) is employed. Rayleigh scattering correction takes care of the shape factor at frequencies higher than 10GHz. The parameters needed to compute the bistatic cross-section (σ_{bi}) for deformed raindrops (for thunderstorm rain type) in tropical locations are stated in Ajewole et. al, (1999). The attenuation occurring on the bistatic link is approximated to consist essentially of attenuation along the path from the transmitting station to the common volume and from the common volume to the earth station receiver in the region below h_{FR}, even though this is very small (Ajewole, et al, 1999). The main contributions are rain and atmospheric gases (Oxygen and water vapour). While the 3D algorithm used utilized the ITU-R recommended procedure for computing attenuation due to atmospheric gases, rain attenuation along the path is computed using the power law relationship of Olsen (1993). The basic input parameters used in

the process of evaluating the cumulative distribution of transmission loss due to interference in this study are as follows;

2.5.1 Link geometry

This study assumed that the path length varies from 50-250Km from terrestrial station to the common volume distance.

2.5.2 Electrical characteristics of the link

The satellite earth station terminal is defined as the interfered station. Its antenna is assumed to have a Gaussian radiation pattern and has a gain set at 59dB, beam width of 0.18°, efficiency of 55%, and elevation angle of 55° which is the look angle of most satellite receiver system over the Atlantic Ocean region in Nigeria. The interfering terrestrial system for this study has an elevation angle of 1°, beam width of 1.6° and antenna gain which varies from 35-55dB.

The antennas are assumed located on the ground, with relative height difference of zero. This assumption allows the lower half of the terrestrial station radiation pattern to be cut off, thus making no contribution to interference. The cumulative distribution of transmission loss is evaluated in the forward direction. The frequency range of interest is 4-35GHz, and the parameters for evaluating the power-law expression for thunderstorm rain type is assumed.

2.5.3 Meteorological parameters

Convective tropical rains are usually generated within the cumulonimbus clouds and can consist of many active centres with strong up-and down drafts. They are also usually characterized by high rainfall intensity and are sometimes accompanied by thunderstorm.

CHAPTER THREE

RESULTS AND DISCUSSION

In this report, the simplified Capsoni 3-Dimensional rain cell model has been used to estimate the statistics of the transmission loss for a horizontally polarized signal transmission over a propagation path length ranging from about 50-250km. The calculation of the common volume (CV) distance to the terrestrial transmitter and receiver respectively, the height of the common volume usually obtained only once for a geometry irrespective of the other input parameters.

3.1 Variation of transmission loss with percentage of time

The results of the cumulative distribution of the transmission loss with percentages of time occurrence ranging from 10^{-5} to10^{-1} % at various frequencies, terrestrial antenna gain of 45 dB and terrestrial antenna station to common volume distance of 50 km is presented in figure 3.1, while figure 3.2 shows the variation for long path length of 200 km. For path length of 50 km, the transmission loss curves varies from about 113.76 to 141.58 dB while for long path lengths of 200 km the transmission loss values varies from 153.4 to 169.83 dB. Over the 50km path-lengths and at a frequency of 34.8GHz, the transmission loss is significantly higher than at other frequencies investigated due to the strong path length attenuation in addition to rapidly decreasing radar reflectivity in the ice region. At frequency 10GHz, there is contribution of rain and other atmospheric gases' attenuation effect on the wanted signal. Transmission loss is greater than that at 16GHz because of the effect of the contribution due to radar reflectivity factor but frequency of 16GHz is not included. So, the contribution of rain and other atmospheric gases effect on the wanted signal make the transmission loss at frequency 10GHz to be greater.

3.2 Comparison of transmission loss for varying terrestrial station to common volume distance

The influence of varying the cumulative distribution of transmission loss with terrestrial propagation paths at time percentages of 10^{-5} to 10^{-1}%, frequency of 16 GHz and terrestrial station antenna gain of 45 dB is presented in figure 3.3. The result shows that the transmission loss increases gradually with increasing antenna separation. This implies less interference at the satellite receiving system. At station separation longer than 170 km, the slope of the curve of transmission loss for the various percentages of time becomes very steep due to the decrease in radar reflectivity factor in the ice region. The common volume is in the ice region, hence ice scattering is dominant.

This case is a bit different when compared with the results of the estimation of intersystem interference on vertically polarized signals as reported by Ajewole, (2003) and Ajewole and Ojo, (2005b). In their report, the steepness of the slope was observed at station separation longer than 200 km. However, the model could not produce result for path lengths longer than 150km at percentage times higher than 0.01%.

Next we examine the influence of varying the transmission loss with the terrestrial station to common volume distance. Figure 3.4 shows this variation for varying TS to common volume CV distance, at frequencies of 8, 10, 16, 20 and 34.8 GHz and time availability of 99.9% (0.01% time unavailability). The result shows that transmission loss increases gradually with increasing antenna separation (less interference) over each of the frequency. Also, the transmission loss at higher frequencies (20 and 34.8 GHz) is significantly higher than at other frequencies due to the larger path

attenuation of the signal. There is also truncation at TS-CV distances greater than 150 km at frequencies 20 and 34.8 GHz for convenience. However, at lower frequency and at distance R_1 greater than 150 km, the contribution from ice begins to dominate because of the blocking effect of the Earth.

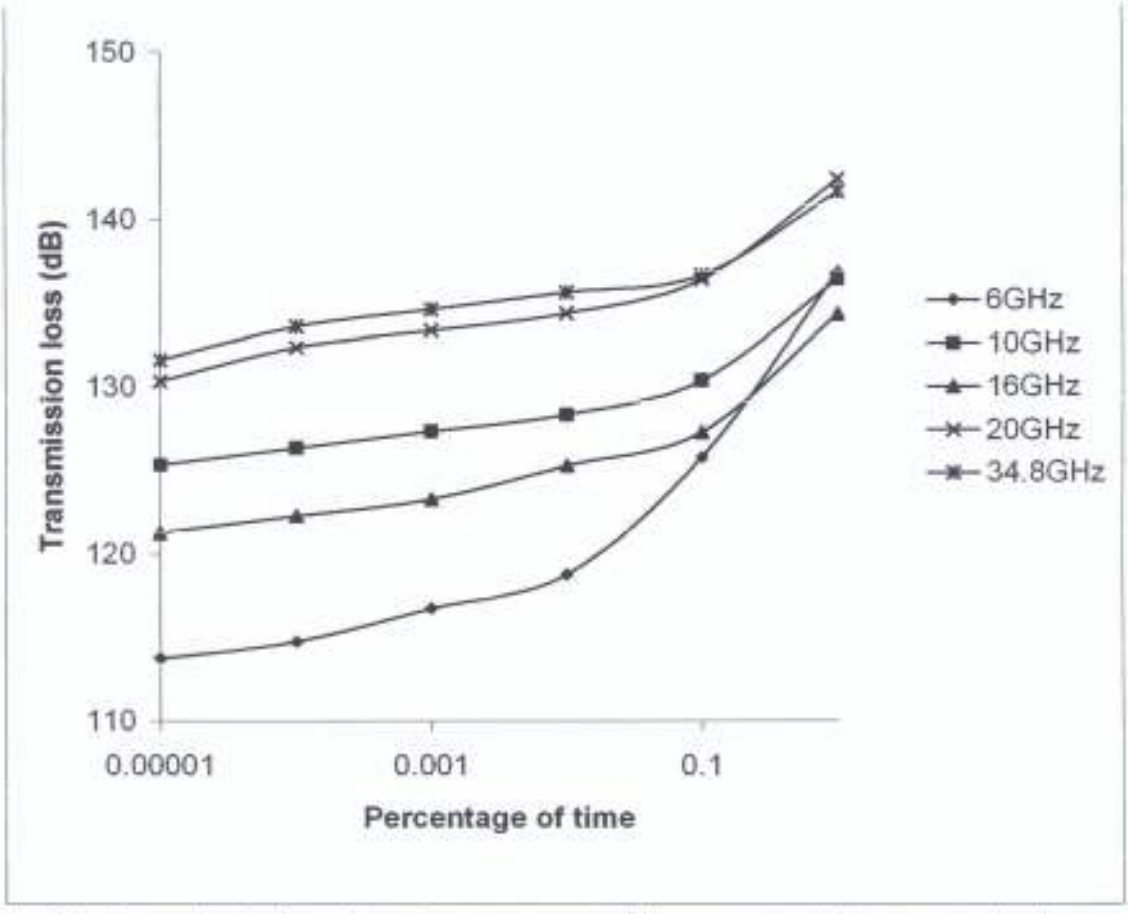

Fig. 3.1: Transmission loss, L against percentage of time at terrestrial antenna gain of 45dB and terrestrial antenna station to common volume distance of 50Km

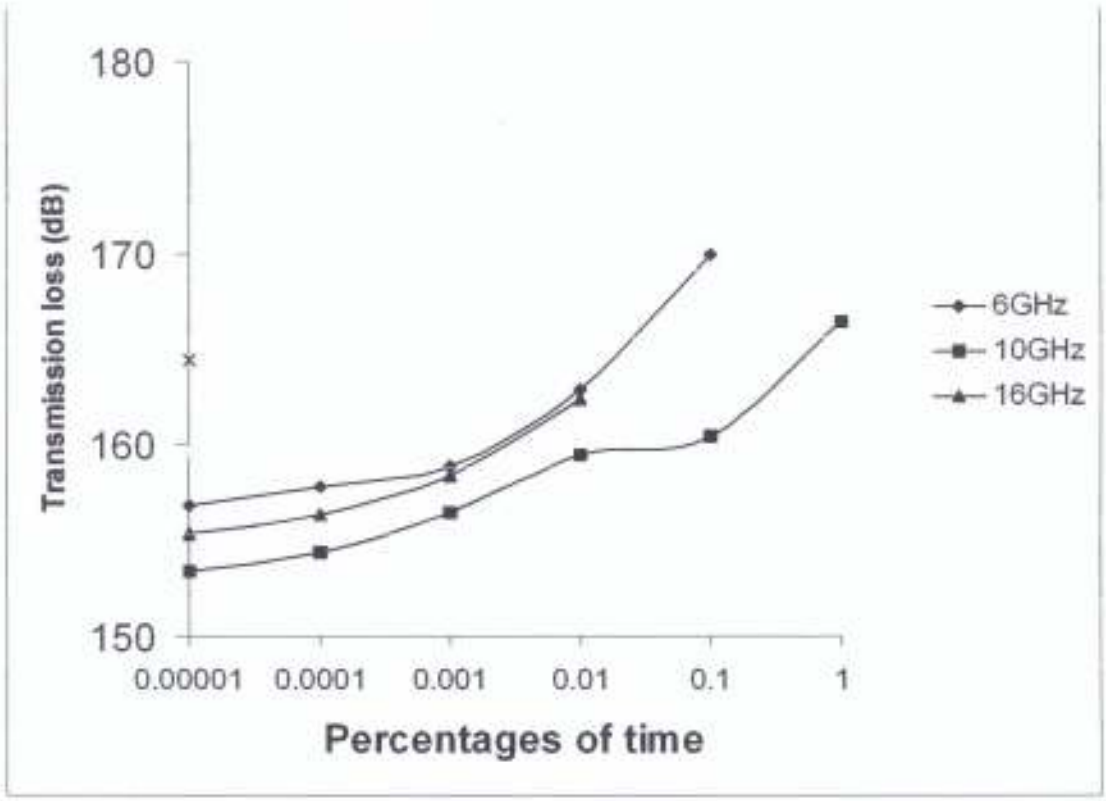

Fig. 3.2: Transmission loss, L against percentage of time at terrestrial antenna gain of 45dB and terrestrial antenna station to common volume distance of 200Km.

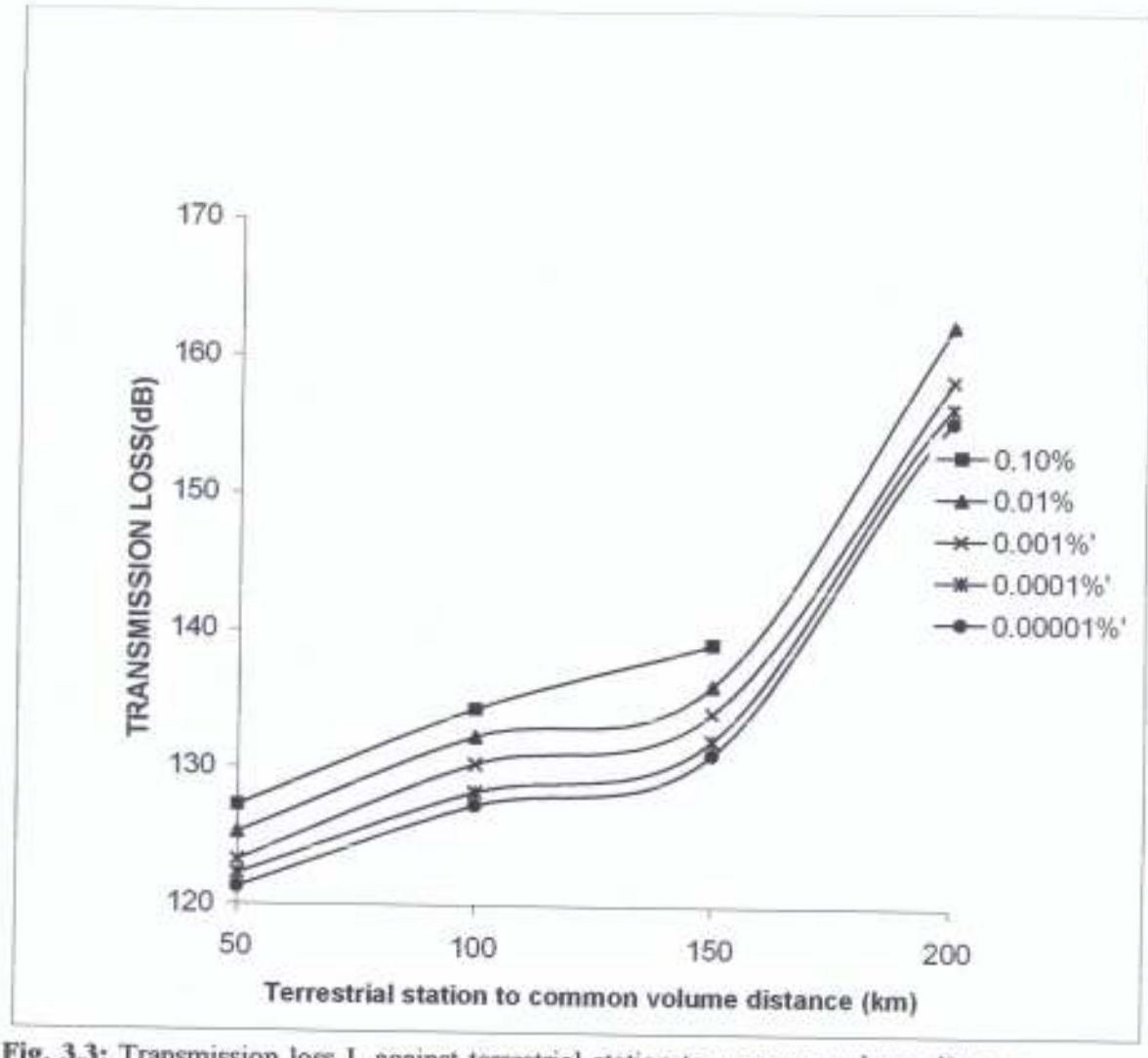

Fig. 3.3: Transmission loss L against terrestrial station to common volume distance (TS- CV) at some percentage of time, frequency of 16 GHz and terrestrial antenna gain of 45 dB

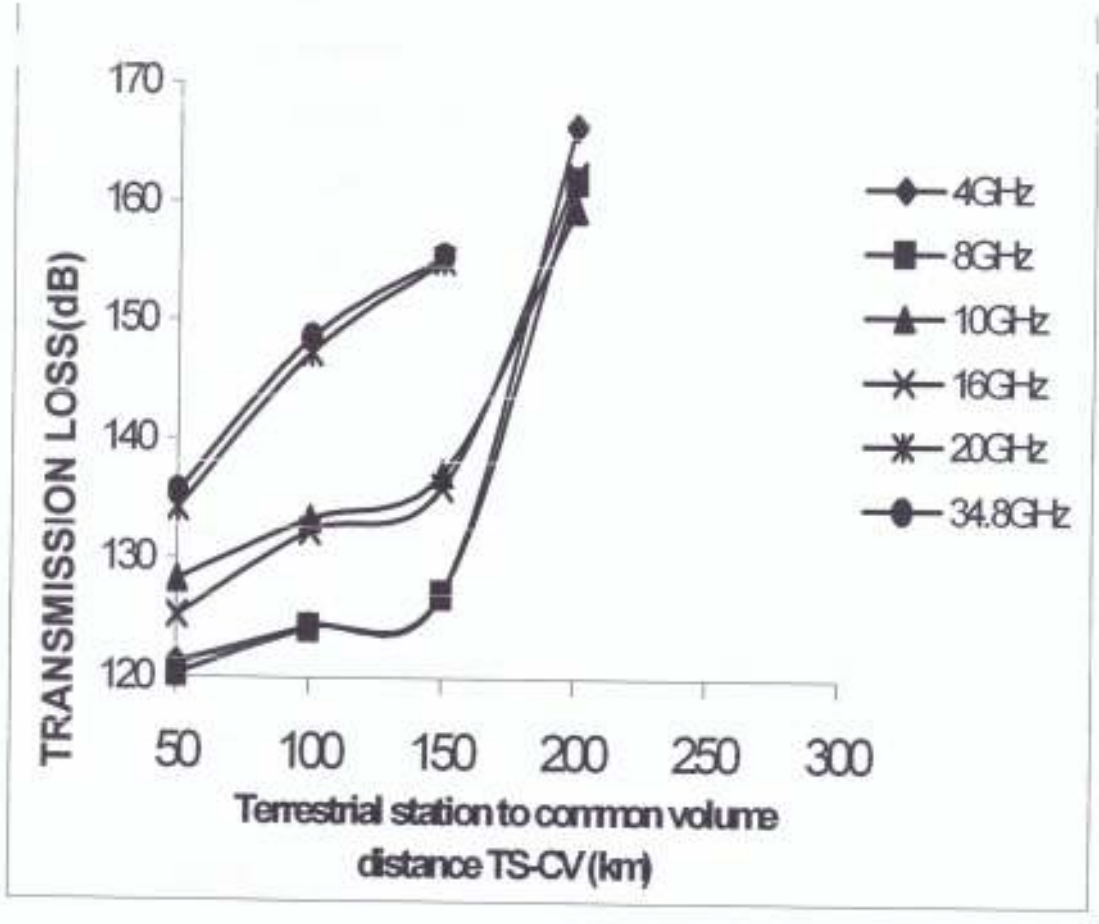

Fig. 3.4: Transmission loss L against terrestrial station to common volume distance (TS- CV) at some frequencies, 0.01% of time and terrestrial antenna gain of 45 dB

3.3 Comparison of the computed transmission loss with frequency

Figs. 3.5 and 3.6 show examples of the cumulative distribution of the transmission loss with frequency for short propagation path length of 50 km and long propagation path length of 200 km respectively at some time percentages. The figures show oscillatory behaviour between 10GHz and 20GHz but rises steadily thereafter to near saturation at frequencies greater than 20GHz. In fig. 3.6 and at higher frequencies, the transmission loss is higher than 160dB at some percentage times. In addition, at frequencies higher than 10GHz, rain attenuation is significant, thus the signal-to-noise ratio in the wanted signal will be very strong as a result of the minimum degradation by the interfering terrestrial signal.

3.4 Comparison of the transmission loss with terrestrial antenna gain.

The variation of the transmission loss is also investigated over terrestrial antenna gain ranging from 35 to 55 dB for horizontally polarised signal passage through thunderstorm rainfall type at time percentages of 10^{-3} to 10^{-1}%. Figures 3.7 to 3.9 show the comparison over short and long path lengths for some frequencies (6 and 20 GHz), the transmission loss at frequencies greater or equal to 20GHz for path lengths higher than 200km is omitted due to an assumption by the algorithm used to discard coupling less than -180 dB for practical purposes. Generally, the results suggest that for a given terrestrial antenna gain, the transmission loss increase with increasing outage probability (decreasing channel availability). Also, the transmission loss decreases linearly with increasing antenna gain for a given outage margin. For example, at frequency of 6 GHz, terrestrial antenna gains varying from 35 to 55 dB and time percentage of 0.01%, the transmission loss decreases from 128.76 dB to 108.76 dB for short path length while it decreases from 172.83 dB to 152.83 dB for long path lengths at the same frequency. Also, at frequency of 20GHz the minimum

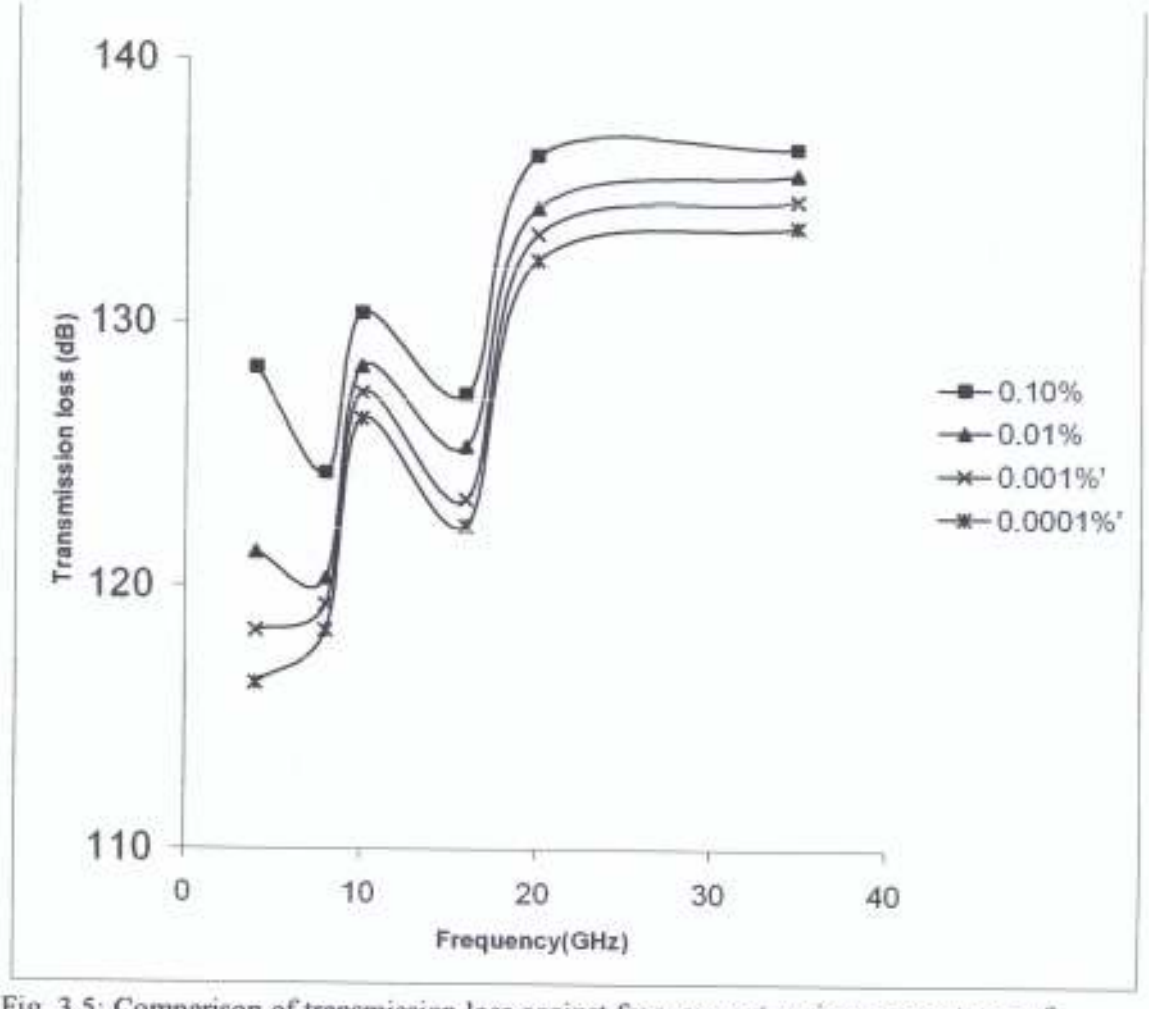

Fig. 3.5: Comparison of transmission loss against frequency at various percentages of time, gain 45dB and station separation 50.7 km.

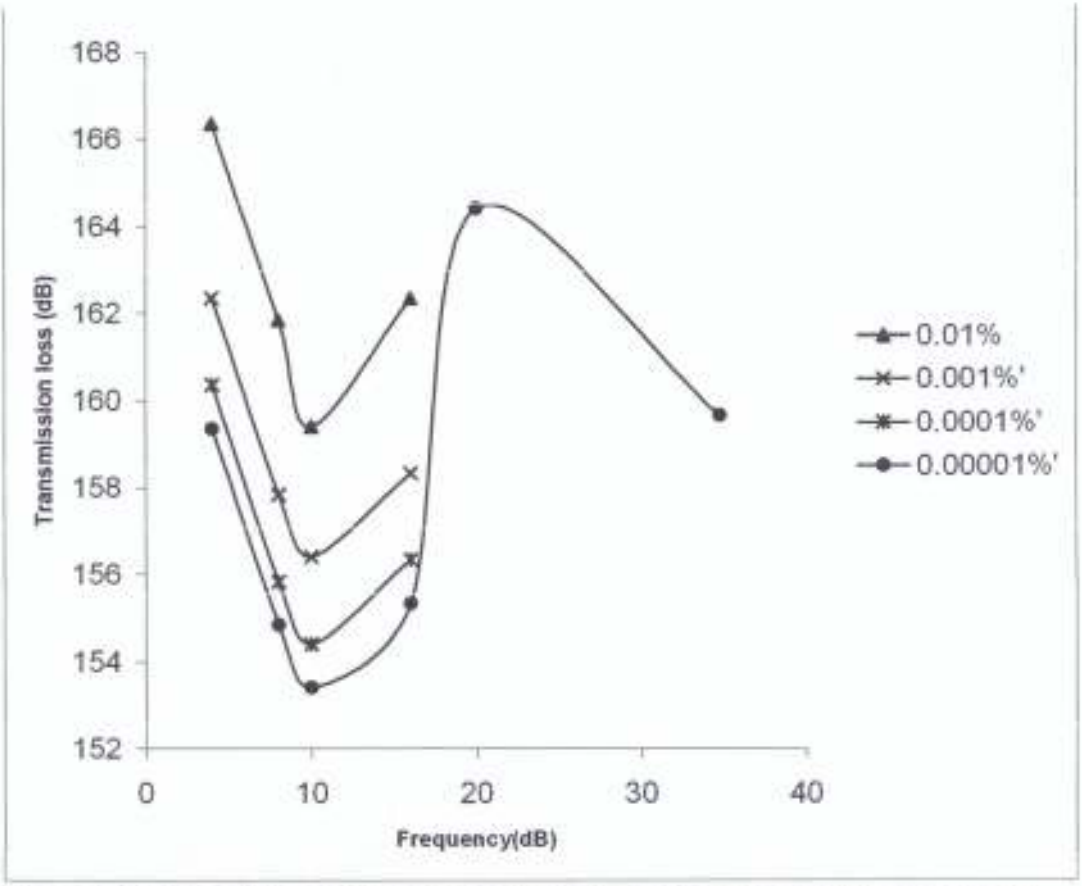

Fig 3.6: Variation of transmission loss with frequency at various percentages of time, gain 45dB and station separation 204Km.

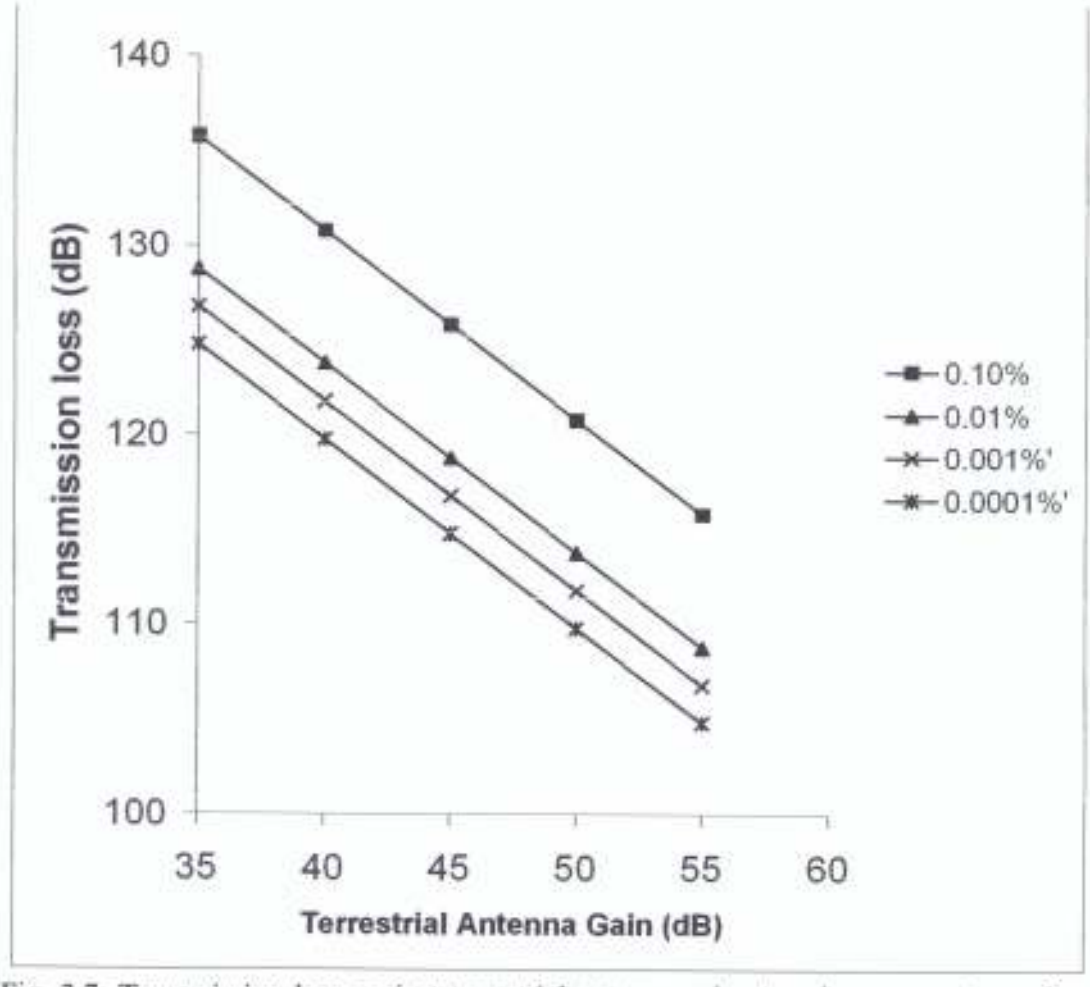

Fig. 3.7: Transmission loss against terrestrial antenna gain at various percentage of time, frequency of 6 GHz and short path length of 50Km.

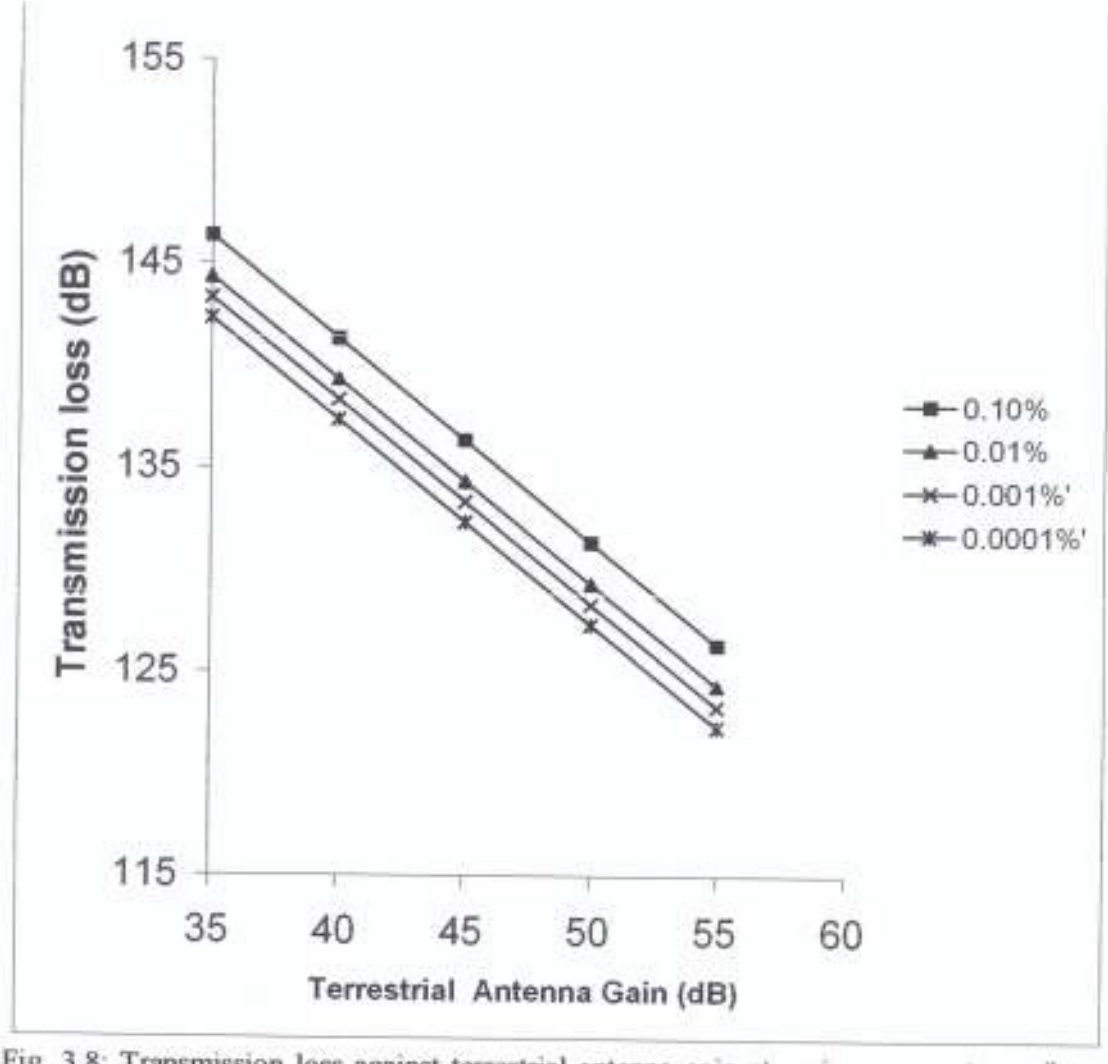

Fig. 3.8: Transmission loss against terrestrial antenna gain at various percentage of time, frequency of 20 GHz and short path length of 50 km.

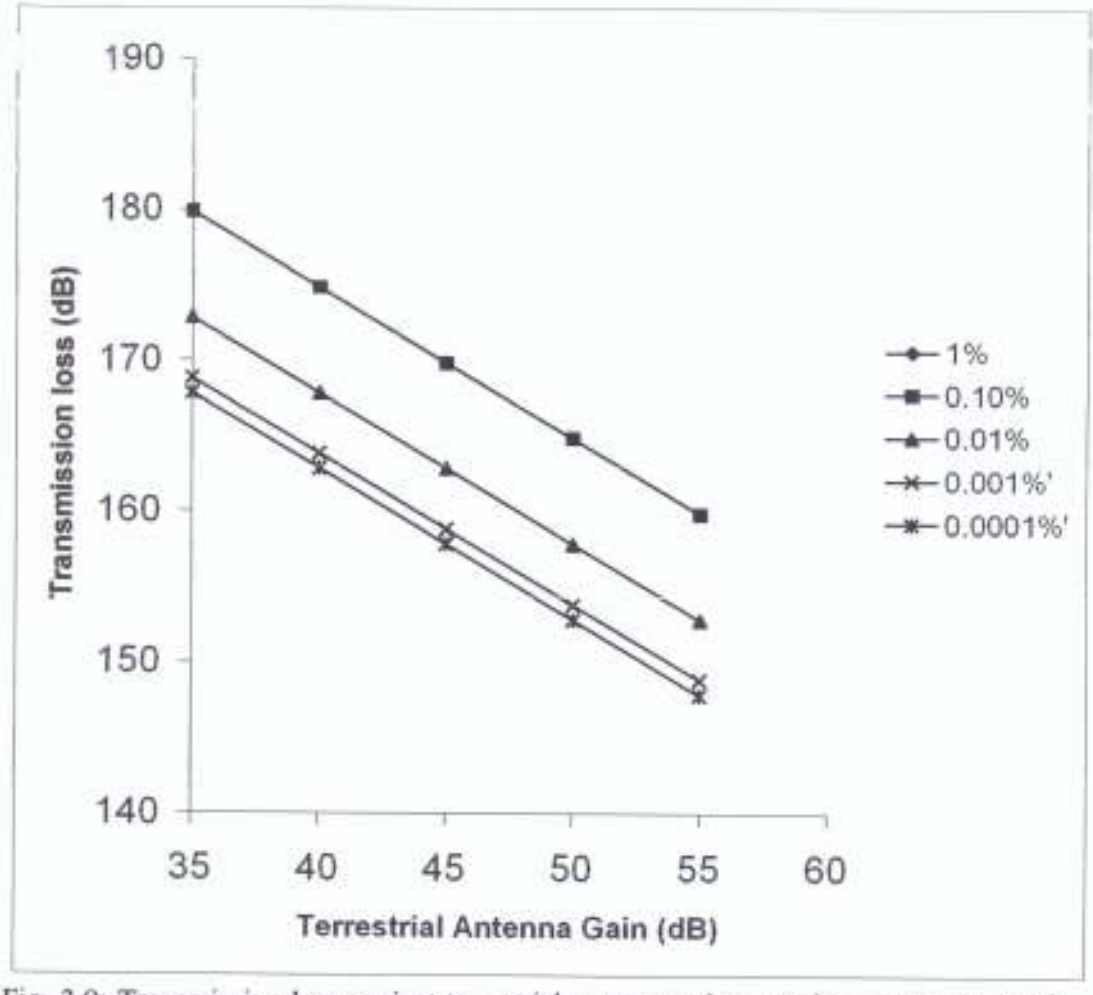

Fig. 3.9: Transmission loss against terrestrial antenna gain at various percentages of time, frequency of 6 GHz and long path length of 200 km.

transmission loss value is 120.33 dB at short path length of 50 km while the model could not produce result for higher time percentages and at frequency greater than 16 GHz due to the practical limit set for the computation for coupling usually around – 180 dB; and so the computation rejects any lower values. Hence there is possibility of severe interference in the satellite receiver at the short separation between the antenna systems, more so that the total attenuation is small at lower frequencies. Also, at long path length of 200 km, the common volume is above the freezing height level, indicating that attenuation due to the ice-region also contributed to this interference.

3.5 Computation of effective transmission loss, Le

This section also considers some possible effects of the extra-attenuation on the horizontally polarized signal transmission. The statistics of the cumulative distribution of transmission loss alone cannot be sufficient to assess the severity of interference at the interfered station when considering interference by rain scatter. At frequencies above about 10 GHz, the wanted signal also suffers attenuation due to hydrometeor scatter, in addition to signal degradation due to depolarization effects. According to Capsoni and D'Amico, (1997), in the locations with intense rain activity, the attenuation along the wanted path could be larger than the maximum link margin so that the satellite link would be out of service whatever the level of interference. However, the signal to noise (S/N) ratio in the receiver terminal can also be reduced by the extra attenuation by rain even when the link margin is not exceeded. Effective transmission loss, Le, is defined as the difference between the transmission loss and the extra attenuation, on the basis of joint dependence on the statistics of the transmission loss and the attenuation. Some parameters are varied with the effective transmission loss in the preceding sub-section.

3.5.1 Comparison of the effective transmission loss Le, with the terrestrial station to common volume distance

The results of the effective transmission loss at some station separation and percentages of time ranging from 10^{-3} to 10^{-1}%, frequency of 16 GHz and terrestrial station gain of 45 dB are presented in figure 3.10. The effective transmission loss ranges from 114.28 dB to 127.26 dB for station separation of 50.7km (TS-CV of 50 km) while it ranges from 156.33 dB to 166.33 dB for long path length of 204 km (TS-CV distance of 200km). The effect of the extra attenuation due to rain along R_2 is quite significant. Generally speaking, Le increased with increasing antenna separation.

The result of the influence of station separation on effective transmission loss at some frequencies for 0.01% of time is as presented in fig. 3.11. At station separation of 50.7 km(TS-CV distance of 50km) and frequency of 6 GHz, Le is about 127.28 dB. The difference between the effective transmission loss is large when compared at lower frequencies and short station separations. Regardless of the frequency, Le is lower at short path length when compared with other path length. This means that there is stronger interference effect due to large increase in attenuation along the short path length. Also, the cumulative distribution of Le shows a significant dependence on the local meteorological point rain rate distribution. Figs. 3.12 and 3.13 show the comparison of the results of Le at some frequencies and percentage of time unavailability for both short and long path lengths. Le decreases slightly with a crest around 20 GHz frequencies. It later decreases after 20 GHz. The effective transmission loss increases with increasing percentages of short time for short path length (50km). However, at long path length, Le decreases up to 10 GHz, but started

increasing at the frequency of 16 GHz, this is due to the decrease in radar reflectivity factor in the ice region and the strong path length attenuation.

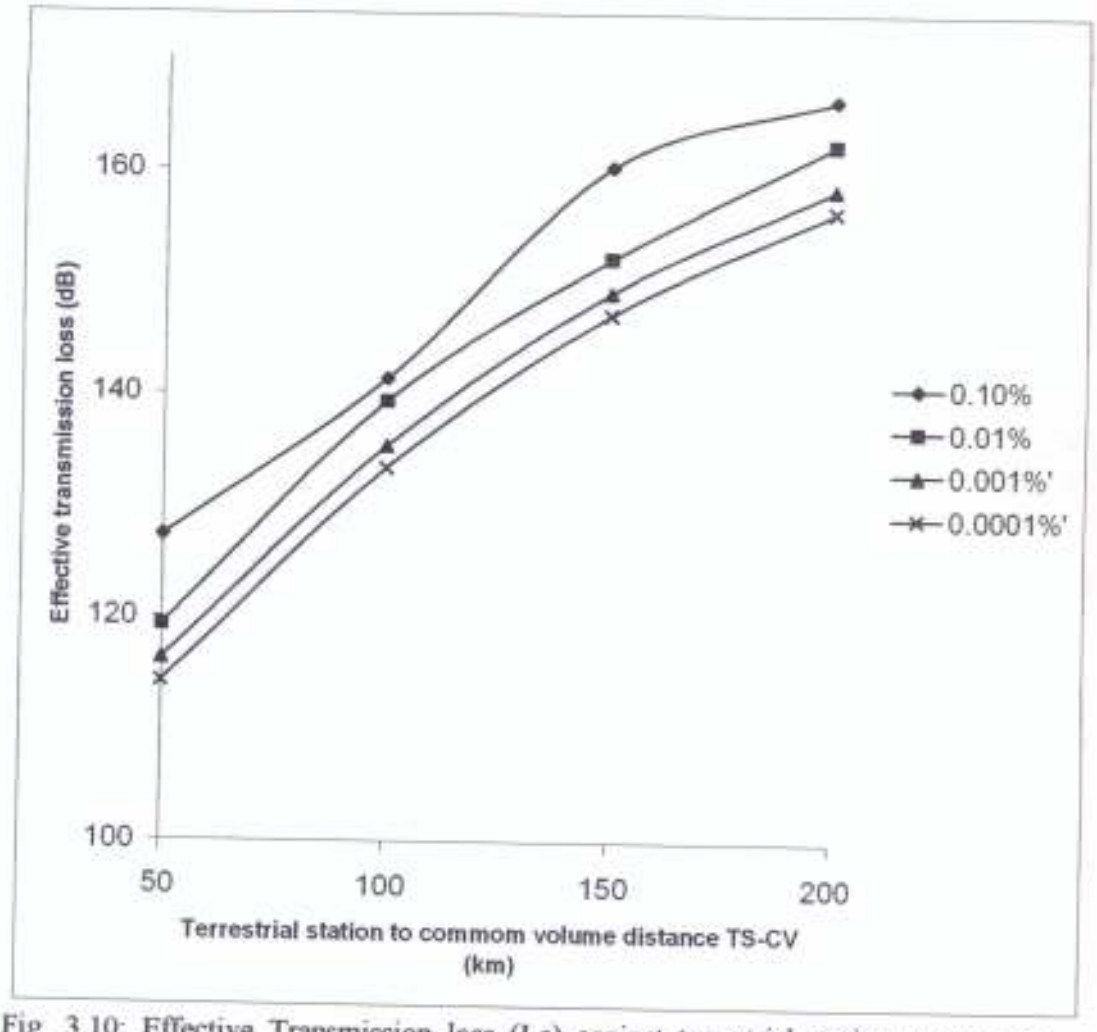

Fig. 3.10: Effective Transmission loss (Le) against terrestrial station to common volume (TS-CV) at various percentage of time.

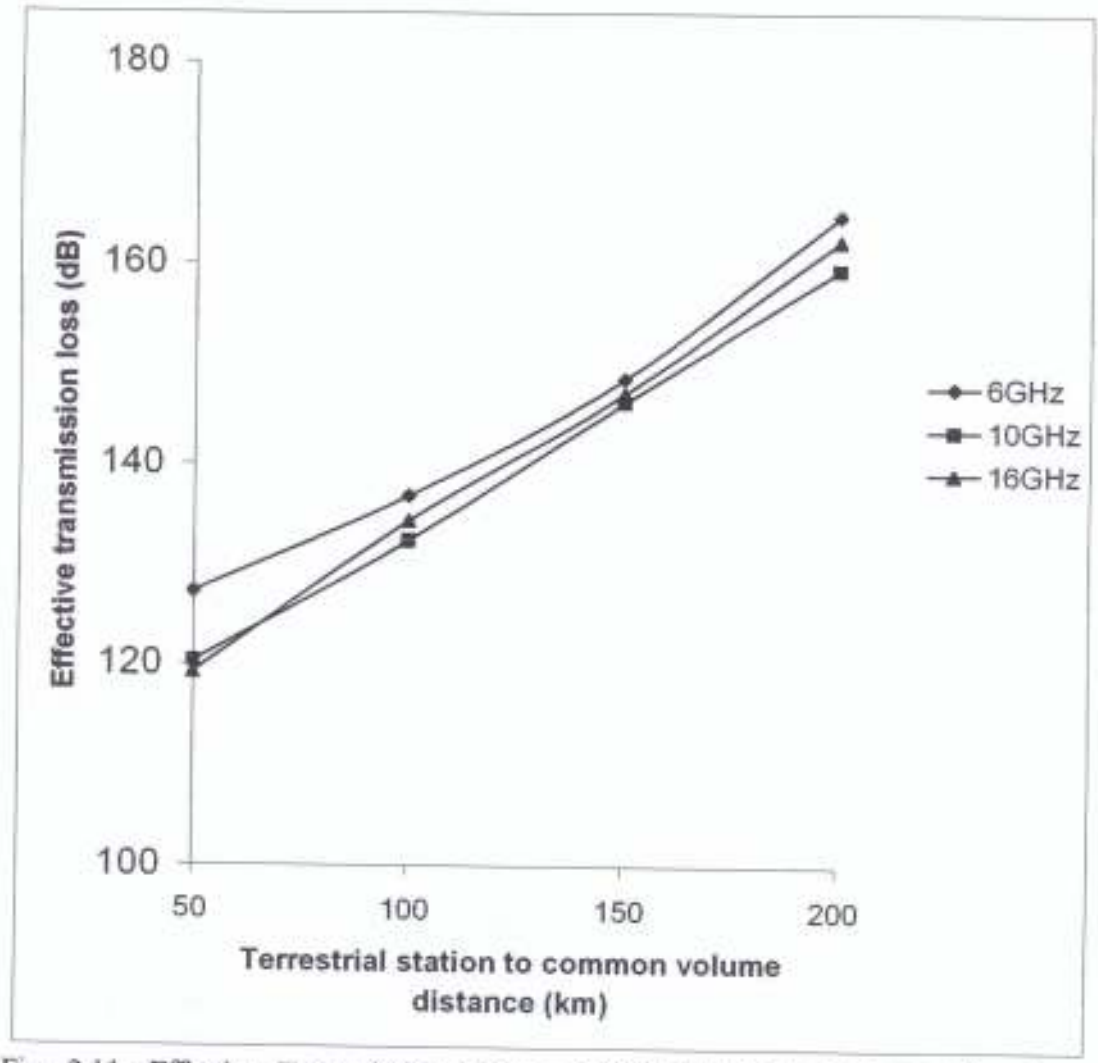

Fig. 3.11: Effective Transmission loss Le against terrestrial antenna station to common volume at various frequencies, antenna gain of 45dB and 0.01 percentage of time.

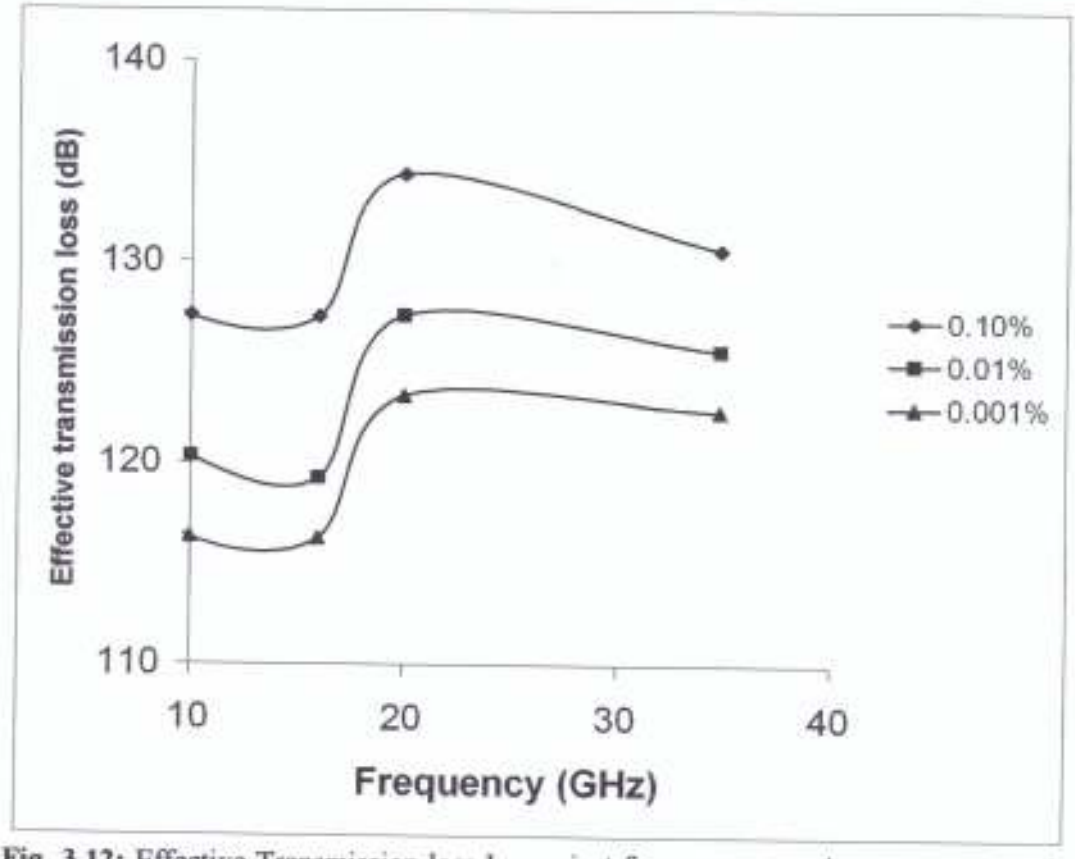

Fig. 3.12: Effective Transmission loss Le against frequency at various percentage of time and at short distance of 50Km.

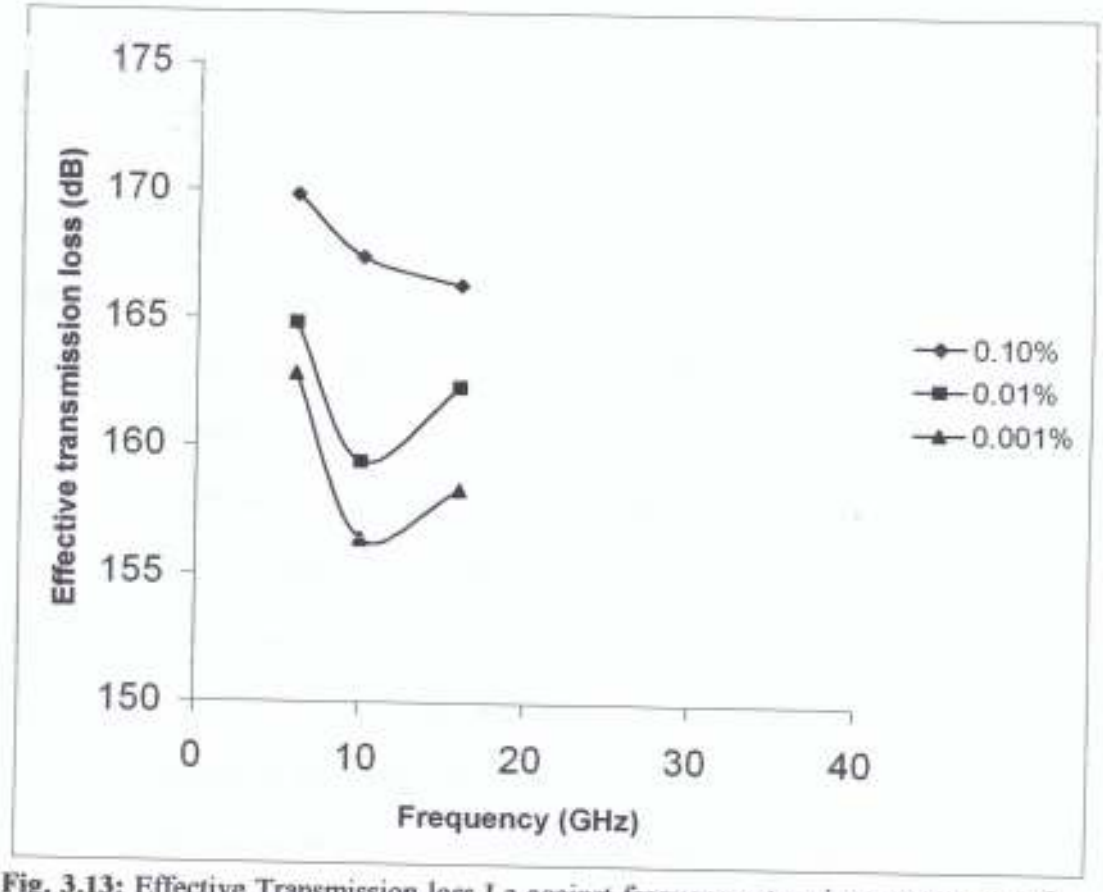

Fig. 3.13: Effective Transmission loss Le against frequency at various percentage of time and at long distance of 200Km.

3.5.2 Comparison of the effective transmission loss with terrestrial antenna gain

The results of the influence of terrestrial antenna gain on the effective transmission loss at some frequencies over short and long path lengths are also presented in figs. 3.14 and 3.15. The time percentage of occurrence ranges from 10^{-3} to 10^{-1}% and terrestrial antenna gain also varies from 35-55 dB. Generally, for a given terrestrial antenna gain, the effective transmission loss increases with increasing time probability. At the same time, Le decreases linearly with increasing antenna gain for a given outage margin. For short path length, Le decreases to a level of 108.27 dB while it decreases to about 147.34 dB for a long path length of 200 km. At 10^{-3} to 10^{-1}% of time, the difference between Le is about 10dB at lower frequency of 6GHz at short path length, while it is about 8dB at the same frequency at long path length. However, higher frequency is not present here because the model will not produce for higher time percentage due to the practical limit set for the computation.

3.5.3 Variation of the effective transmission loss with percentage of time

Figures 3.16 and 3.17 shows the result of the comparison of the effective transmission loss with percentages of time over short and long terrestrial propagation paths respectively. The comparison was made at frequencies of 6, 10, 16 and 34.8 GHz. The effect of the extra attenuation due to rain along R_2 is quite significant. Though not shown in this report, the extra attenuation is more pronounced at long path length when compared with short path length. This result is in good agreement with the earlier work of Ajewole and Ojo, (2005b).

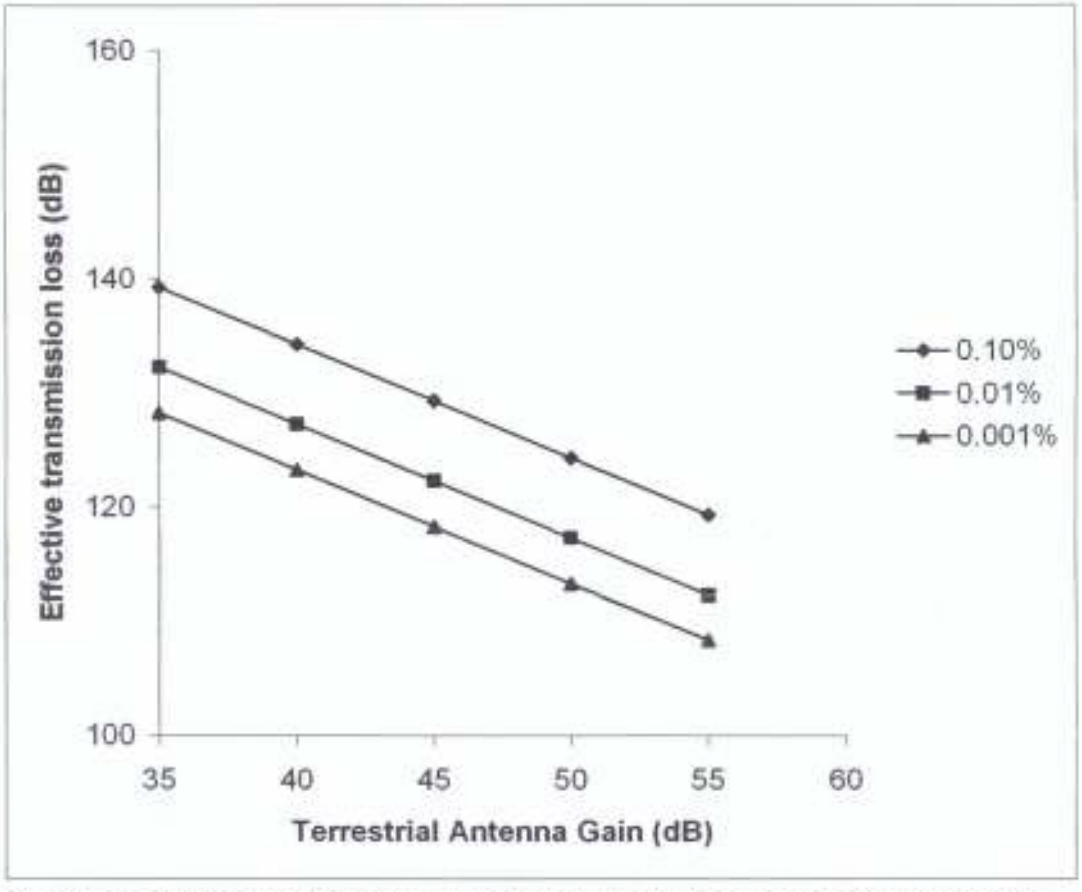

Fig. 3.14: Effective Transmission loss Le against terrestrial antenna Gain at frequency 6GHz and short distance of 50Km.

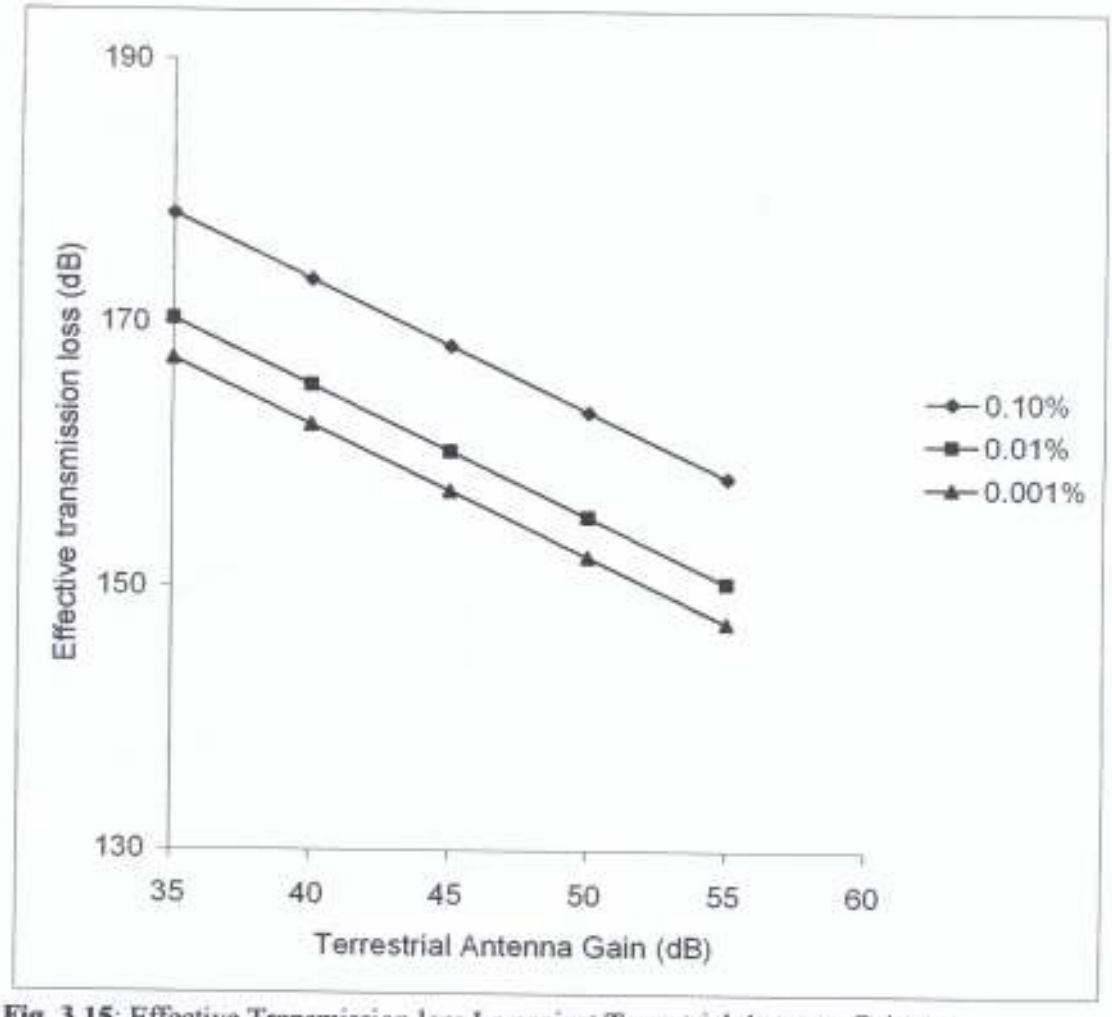

Fig. 3.15: Effective Transmission loss Le against Terrestrial Antenna Gain at frequency 6GHz and long distance of 200Km.

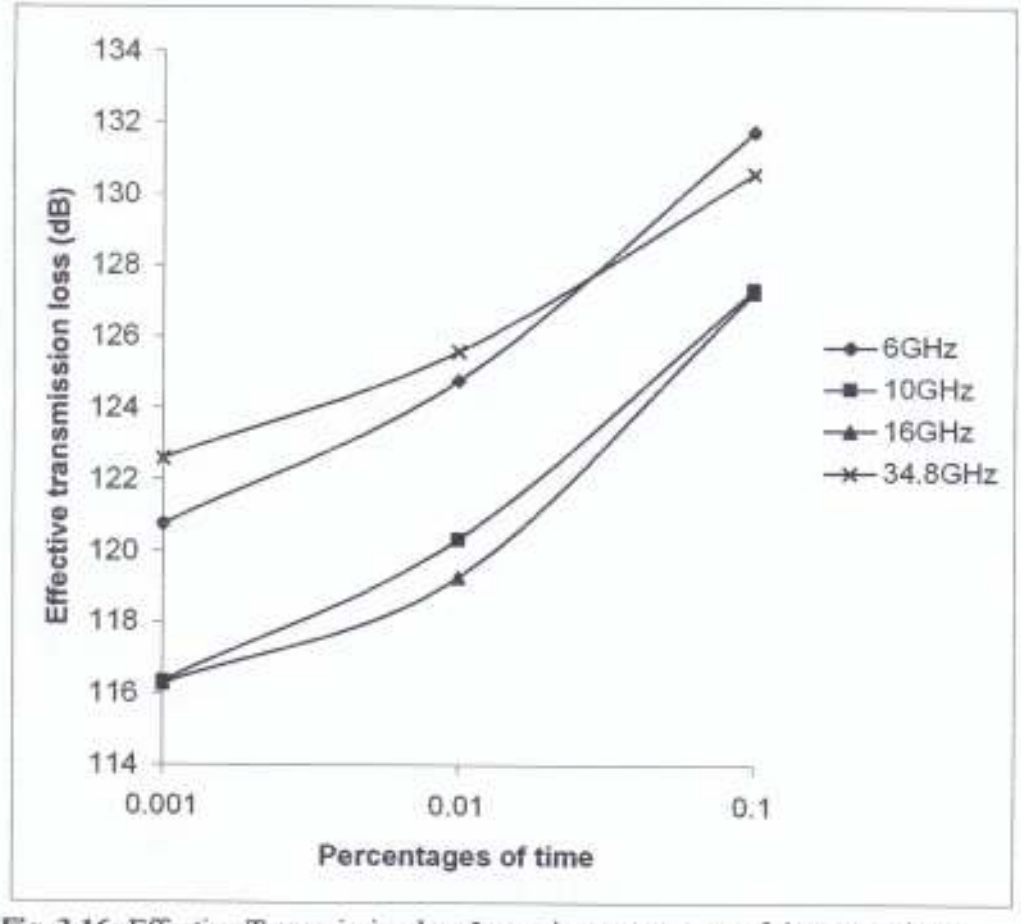

Fig. 3.16: Effective Transmission loss Le against percentage of time at various frequencies and at short distance of 50Km.

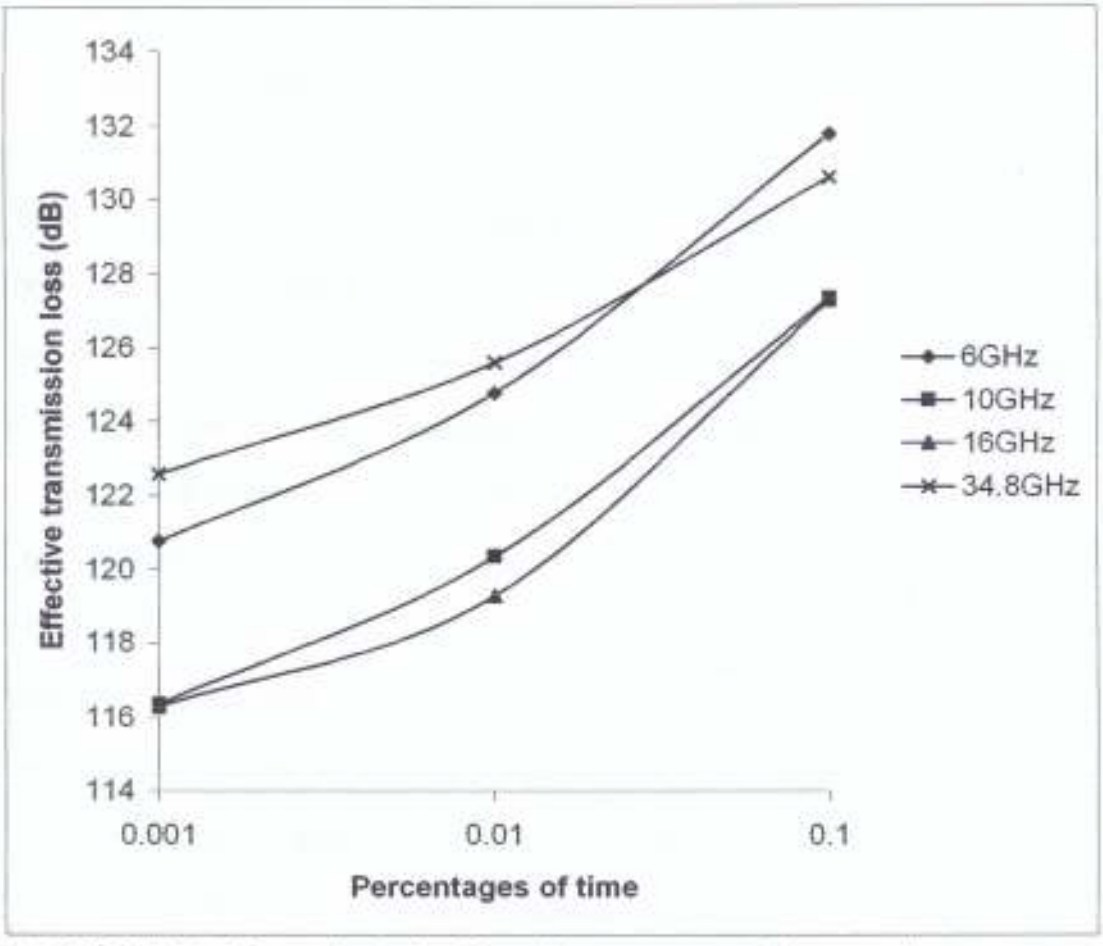

Fig. 3.17: Effective Transmission loss Le against percentage of time at various frequencies and at long distance of 200Km.

CHAPTER FOUR

4.1 CONCLUSION

In this report, the simplified 3D bistatic radar equation has been employed to calculate intersystem interference (transmission loss) L, and the effective transmission loss, Le for horizontally polarized signal propagation through thunderstorm rainfall type. The results have been presented by analysing parameters such as frequency dependence, terrestrial station antenna gain; antenna separations among others and their effects on transmission loss have been investigated. The results of the transmission loss with varying station separation obtained in this report are in good agreement with similar ones obtained by Ajewole and Ojo, (2005a), Ajewole and Ojo, (2005b), Ajewole, et al (1999) and Ajewole, (2003) for a vertically polarized signal transmission. The frequency characteristics of the transmission loss L, for 45 dB gain and occurrence time percentage of 0.01% shows that it varies from 121.28 dB to 135.58 dB for short path lengths while it varies from 159.4 to 166.35 dB long path length. It should be noted however that some common assumptions were made for the stations in the evaluation process, such as similar h_{FR} height, rainfall and meteorological parameters among others. The evaluation of the effective transmission loss shows that additional rain attenuation will severely weaken the received signal, which may lead to acute outage during occurrence of heavy and intense tropical precipitation. The results of the present work are in good agreement with those of the previous researchers particularly for Nigeria. However, the results require experimental validation; notwithstanding, the information will still serve as a database in the planning of an acceptable satellite communications networks utilizing a horizontally polarized signal in Nigeria.

4.2 RECOMMENDATION

As the communication networks are growing in the country, it is required that much research should be carried out using appropriate parameters to obtain more data for planning effective communication networks for the nation. However, it may not be easy to carry out such studies as it requires up-to-date instrumentation and substantial funding.

Funding should therefore be provided by the government and the communication industries for research to enhance better telecommunication services.

REFERENCES

Ajayi, G.O and Owolabi, I.E. (1987): Rainfall parameters from distrometer drop size measurements at a tropical station. *Ann. Telecomm.* Vol. 42 No 1-2, Pp 4-12.

Ajayi, G.O. and Barbaliscia, F (1990): Prediction of attenuation due to rain characteristics of the 0oC isotherm in temperate and tropical climates. *Int. J. Satellite comm.*, Vol. 8, Pp 187-196.

Ajewole, M.O, Kolawole, L.B. and Ajayi, G.O (1999): Evaluation of bistatic intersystem interference due to scattering by hydrometeor on tropical paths, *Int. J. satellite comm.*. Vol. 17, Pp 339-356.

Ajewole, M.O. (2003): Bistatic interference due to tropical rainfall types: a comparison of rain-cell models, *Atti Della Fondazione Giorgio Ronchi*, Vol. 58, No 1, pp 129-141.

Ajewole, M.O. and Ojo, J.S. (2005a): Comparative study of Bistatic intersystem interference in low latitude tropical location. *Journal of research in science and management* 3(1), 41-49.

Ajewole, M.O. and Ojo, J.S. (2005b): Intersystem interference due to hydrometeor scattering on satellite down link signal in tropical location. *African journal of science and technology, UNESCO (AJST),* 6(2), 84-93.

Awaka, J and Oguchi, T. (1982): Bistatic radar reflectivities of Pruppacher-Pitter form raindrops at 34.8GHz. Radio Sci. Vol. 17, No 1, pp 269-278.

Capsoni, C and D'Amico, M (1997): A physically based simple prediction method for scattering interference. *Radio science.* Vol. 32, No 2 Pp 397-407.

Capsoni, C., Fedi, F, Magistroni, C, Paraboni, A and Pawlina, A. (1997): Data and theory for a new model of the horizontal structure of rain cells for propagation applications. *Radio Sci.* vol. 22, No 3, Pp 395-404.

Commission of the European Communities on Cooperation in the fields of Scientific and Technical research, COST 210: Influence of the atmosphere on interference between radio communication systems at frequencies above 1GHz, Final Rept, EUR 13407EN, Brussels, 1991.

Crane, R. (1974): Bistatic scatter from rain, *IEEE Trans. Ant. and Propag;* A P 22 (2), Pp312-320.

International Telecommunication Union and Radio Communication ITU-R (1999): Characteristics of precipitation for propagation modelling. Geneva. P 837-2.

Medeiros Filho, F.C, Cole, R.S. and Sarma, A.D. (1986): Millimetre wave rain induced attenuation theory and experiment. IEEE Proc. Vol. 133 Pt. H, No 4 Pp 308-314.

Mismie, P and Waldteufel, P (1980): A model for attenuation by precipitation on a microwave earth-space link. Radio Sci. Vol. 15, Pp 655-665.

Olsen, R.L. (1993): Interference due to hydrometeor scatter on Satellite communication links. Proc. IEEE, Vol. 81, No 6 Pp914-922.

Ray, P .S (1972): Broadband complex refractive indices of ice and water, *Applied Optics*, Vol. 11, No. 8, Pp1836-1844.

Thurai, M. (1994): Climatic parameters required for the prediction of interference due to precipitation scatter.